Asian Journal of Control, Vol. 21, No. 4, pp. 1–12, July 2019
Published online in Wiley Online Library (wileyonlinelibrary.com) DOI: 10.1002/asjc.1808

REDUCED-ORDER OBSERVER FOR STATE-DEPENDENT COEFFICIENT FACTORIZED NONLINEAR SYSTEMS

Fernando Ornelas-Tellez, Alma Y. Alanis, Jorge D. Rios and Mario Graff

ABSTRACT

This paper presents a reduced-order observer for state-dependent coefficient factorized nonlinear systems. By considering that a partial knowledge of the state vector is available from measurements, estimating the full state vector may be unnecessary, which consequently reduces the order of the observer and thus avoids unnecessary implementation issues. In this manuscript, the asymptotic convergence of the proposed reduced-order observer is established when an adequate state-dependent factorization for the nonlinear system is obtained. This paper demonstrates the ease of synthesizing reduced-order observers for state-dependent coefficient factorized nonlinear systems. The effectiveness of the proposed observer is illustrated in real-time for the optimal tracking control of a linear induction motor.

Key Words: Reduced-order observer, state-dependent coefficient factorized nonlinear systems, nonlinear optimal tracking control, linear induction motor.

I. INTRODUCTION

For control systems, in order to obtain high performance from a synthesized controller, knowledge of the system model is usually required, where the state variables involved in the system are used for feedback. Hence, under this condition, it is assumed that the full state variables are available for feedback; however, in practice, when the full state vector is not accessible from measurements, synthesizing a state observer in order to estimate the missing state variables is necessary. This estimation can be derived from the synthesis of a full-order observer (when the order of the observer is the same as the system) or a reduced-order observer (when the order of the observer is less than the system). State estimation has been studied by many authors, who have obtained a range of interesting results [1–6]. In particular, this paper considers the reduced-order observer scheme, which results from assuming that we have partial knowledge of the state vector. Therefore, it could be unnecessary to estimate all of the state vector, leading to the synthesis of an observer of order $n-q$, where n is the order of the system and q is the number of the available state variables from measurements.

This paper proposes a methodology for the synthesis of a reduced-order observer for the class of state-dependent coefficient factorized (SDCF) nonlinear systems. The proposed observer ensures an asymptotic convergence of the estimation error when an adequate factorization of the nonlinear system can be obtained. Various advantages can be exploited for SDCF systems, such as stability analysis, controller design methodologies, observer synthesis, and filter designs [7], among others, which can be analogously designed as developed for linear systems. One of the drawbacks of the SDCF strategy is the non-uniqueness of the factorization, which could mean that selecting an appropriate factorization of large and/or complicated nonlinear systems is a difficult task. Different experimental and practical applications of this SDCF control methodology have demonstrated its effectiveness for a great variety of nonlinear systems [8–15]. A comprehensive survey for SDCF nonlinear systems is presented in [16]. Note that although results regarding state estimation for SDCF nonlinear systems exist [2,3,8,17], the reduced-order observers' synthesis for this class of systems, to the best of our knowledge, has not been analyzed. The applicability of the reduced-order observer synthesis is illustrated and validated in real-time for the observer-based optimal tracking control of a linear induction motor (LIM).

The paper is organized as follows. The synthesis of a reduced-order observer for the class of SDCF nonlinear systems is described in Section II. Section III presents an optimal tracking control scheme for this

Manuscript received January 3, 2018; accepted February 4, 2018.
F. Ornelas-Tellez is with the Faculty of Electrical Engineering, Universidad Michoacana de San Nicolas de Hidalgo, Morelia 58030, Mexico (corresponding author, e-mail: fornelast@gmail.com).
A. Y. Alanis and J. D. Rios are with CUCEI, Universidad de Guadalajara, Blvd. Marcelino Garcia Barragan 1421, Col. Olimpica, 44430 Guadalajara, Jalisco, Mexico (e-mail: almayalanis@gmail.com, jorge_rios.1xyz@yahoo.com).
M. Graff is with INFOTEC, Aguascalientes, Mexico (e-mail:mario.graff@infotec.mx).
This research work is supported by CONACYT, Mexico, under projects CB-222760 and CB-256769 (Proyecto Apoyado por el Fondo Sectorial de Investigación para la Educación). The authors gratefully thank the reviewers and the associate editor for their useful comments and suggestions for improving the paper.

class of nonlinear systems. Section IV presents the real-time implementation and the experimental results of the proposed reduced-order observer-based optimal control scheme for a LIM. Finally, Section V concludes the paper.

II. REDUCED-ORDER OBSERVER FOR SDCF NONLINEAR SYSTEMS

2.1 SDCF nonlinear systems

This section describes the nonlinear systems that can be represented by a state-dependent coefficient factorization and for which the reduced-order observer is proposed.

Let us consider the nonlinear system

$$\dot{x} = f(x) + B(x)\,u, \qquad x(t_0) = x_0 \tag{1}$$

$$y_m = H\,x \tag{2}$$

where $x \in \mathbb{R}^n$ is the state vector, $u \in \mathbb{R}^m$ is the control input and $y_m \in \mathbb{R}^q$ is the vector of the system measured variables; functions $f(x)$ and $B(x)$ are smooth maps of appropriate dimensions, with $f(0) = 0$, and $H \in \mathbb{R}^{q\times n}$ is a constant matrix related to the measured variables.

Consider that $f(x)$ in (1) can be decomposed in the SDCF form [18–20] as $f(x) = A(x)\,x$, then system (1) results in

$$\dot{x} = A(x)\,x + B(x)\,u. \tag{3}$$

As established in [7,21], the assumptions $f(0) = 0$ and $f(\cdot) \in C^1$ allow that the factorization as described in (3) can be carried out. Note that $A(x)\,x$ is not unique [8]. In order to obtain well-defined control schemes, appropriate factorization for these representations should be determined such that controllability and observability properties are fulfilled for systems (2)– (3), which are described in detail in [8,11,18,22].

2.2 Reduced-order observer synthesis

This section proposes a reduced-order observer for estimating only the unmeasured states, which depend indirectly on the available measurements [23–25]. In this case, partitioning the state vector of the system into two groups [4,23] is possible: the available states $\bar{x}_1$ from measurements and the unavailable states $\bar{x}_2$.

Let us assume that H in (2) has a full row rank, that is, $rank\{H\} = q$. Define a matrix

$$T = \begin{bmatrix} H \\ S \end{bmatrix}$$

where S is a $(n-q)\times n$ real matrix, which is selected entirely arbitrarily such that T is nonsingular. By applying the similitude transformation $\bar{x} = Tx$ to system (3), the following transformed system is then obtained:

$$\begin{aligned} \dot{\bar{x}} &= TA(\bar{x})\,T^{-1}\bar{x} + TB(\bar{x})\,u \\ y_m &= H\,T^{-1}\bar{x} \\ &= \begin{bmatrix} I_q & 0 \end{bmatrix}\bar{x} \end{aligned} \tag{4}$$

where I_q is the $q\times q$ identity matrix and $\bar{x} = Tx = \begin{bmatrix} \bar{x}_1^T, & \bar{x}_2^T \end{bmatrix}^T$, the dynamics of which can be partitioned as

$$\begin{bmatrix} \dot{\bar{x}}_1 \\ \dot{\bar{x}}_2 \end{bmatrix} = \begin{bmatrix} A_{11}(\bar{x}) & A_{12}(\bar{x}) \\ A_{21}(\bar{x}) & A_{22}(\bar{x}) \end{bmatrix} \begin{bmatrix} \bar{x}_1 \\ \bar{x}_2 \end{bmatrix} + \begin{bmatrix} B_1(\bar{x}) \\ B_2(\bar{x}) \end{bmatrix} u \tag{5}$$

with

$$y_m = \bar{x}_1 \tag{6}$$

as the system measured variables.

For the transformed system, vector $\bar{x}_1$ contains the first q entries of $\bar{x}$ and $\bar{x}_2$ the remaining ones. Matrices $A_{11}(\bar{x})$, $A_{12}(\bar{x})$, $A_{21}(\bar{x})$, $A_{22}(\bar{x})$, $B_1(\bar{x})$ and $B_2(\bar{x})$ are of appropriate dimensions and accordingly are partitioned from (4).

By using (6), system (5) can be rewritten as

$$\begin{bmatrix} \dot{y}_m \\ \dot{\bar{x}}_2 \end{bmatrix} = \begin{bmatrix} A_{11}(\bar{x}) & A_{12}(\bar{x}) \\ A_{21}(\bar{x}) & A_{22}(\bar{x}) \end{bmatrix} \begin{bmatrix} y_m \\ \bar{x}_2 \end{bmatrix} + \begin{bmatrix} B_1(\bar{x}) \\ B_2(\bar{x}) \end{bmatrix} u. \tag{7}$$

By defining $\bar{u} = A_{21}(\bar{x})\,y_m + B_2(\bar{x})\,u$ and $\varpi = \dot{y}_m - A_{11}(\bar{x})\,y_m - B_1(\bar{x})\,u$, we obtain

$$\begin{aligned} \dot{\bar{x}}_2 &= A_{22}(\bar{x})\,\bar{x}_2 + \bar{u} \\ \varpi &= A_{12}(\bar{x})\,\bar{x}_2. \end{aligned} \tag{8}$$

Therefore, when system (8) is state-dependent observable, then an estimator can be constructed for $\bar{x}_2$ such as

$$\begin{aligned} \dot{\hat{\bar{x}}}_2 &= A_{22}\left(\hat{\bar{x}}\right)\hat{\bar{x}}_2 + \bar{u} + \bar{L}\,(\varpi - \hat{\varpi}) \\ &= A_{22}\left(\hat{\bar{x}}\right)\hat{\bar{x}}_2 + \bar{u} + \bar{L}\left(\varpi - A_{12}\left(\hat{\bar{x}}\right)\hat{\bar{x}}_2\right) \\ &= \left(A_{22}\left(\hat{\bar{x}}\right) - \bar{L}A_{12}\left(\hat{\bar{x}}\right)\right)\hat{\bar{x}}_2 \\ &\quad + \left(A_{21}\left(\hat{\bar{x}}\right) - \bar{L}A_{11}(\bar{x})\right)y_m \\ &\quad + \left(B_2\left(\hat{\bar{x}}\right) - \bar{L}B_1\left(\hat{\bar{x}}\right)\right)u + \bar{L}\dot{y}_m \end{aligned} \tag{9}$$

where $\hat{\varpi} = A_{12}\left(\hat{\bar{x}}\right)\hat{\bar{x}}_2$ and $\bar{L}$ is the estimation error gain used to achieve the estimator convergence.

A suitable change of variable in order to avoid the time derivative of y_m in (9) is realized by defining

$$\bar{z} = \hat{\bar{x}}_2 - \bar{L}\,y_m \tag{10}$$

and thus

$$\begin{aligned}\dot{\hat{z}} &= \left(A_{22}\left(\hat{\bar{x}}\right) - \bar{L}A_{12}\left(\hat{\bar{x}}\right)\right)\left(\bar{z} + \bar{L}y_m\right) \\ &\quad + \left(A_{21}\left(\hat{\bar{x}}\right) - \bar{L}A_{11}\left(\hat{\bar{x}}\right)\right)y_m \\ &\quad + \left(B_2\left(\hat{\bar{x}}\right) - \bar{L}B_1\left(\hat{\bar{x}}\right)\right)u.\end{aligned} \tag{11}$$

Hence, from (10), an estimate for $\bar{x}_2$ is given by

$$\hat{\bar{x}}_2 = \bar{z} + \bar{L}y_m. \tag{12}$$

In order to analyze the stability of the reducer-order observer, let us consider the estimation error as

$$e = \bar{x}_2 - \left(\bar{z} + \bar{L}y_m\right) \tag{13}$$

where its time derivative results in

$$\begin{aligned}\dot{e} &= \dot{\bar{x}} - \left(\dot{\bar{z}} + \bar{L}\dot{y}_m\right) \\ &= A_{22}(\bar{x})\bar{x}_2 + A_{21}(\bar{x})y_m + B_2(\bar{x})u \\ &\quad - \left(A_{22}\left(\hat{\bar{x}}\right) - \bar{L}A_{12}\left(\hat{\bar{x}}\right)\right)\left(\bar{z} + \bar{L}y_m\right) \\ &\quad - \left(A_{21}\left(\hat{\bar{x}}\right) - \bar{L}A_{11}\left(\hat{\bar{x}}\right)\right)y_m \\ &\quad - \left(B_2\left(\hat{\bar{x}}\right) - \bar{L}B_1\left(\hat{\bar{x}}\right)\right)u \\ &\quad - \bar{L}A_{11}(\bar{x})y_m - \bar{L}A_{12}(\bar{x})\bar{x}_2 - \bar{L}B_1(\bar{x})u \\ &= \left(A_{22}(\bar{x}) - \bar{L}A_{12}(\bar{x})\right)\bar{x}_2 \\ &\quad - \left(A_{22}\left(\hat{\bar{x}}\right) - \bar{L}A_{12}\left(\hat{\bar{x}}\right)\right)\left(\bar{z} + \bar{L}y_m\right) \\ &\quad + \Big[\left(A_{21}(\bar{x}) - A_{21}\left(\hat{\bar{x}}\right)\right) + \\ &\bar{L}\left(A_{11}\left(\hat{\bar{x}}\right) - A_{11}(\bar{x})\right)\Big]y_m \\ &\quad + \left[\left(B_2(\bar{x}) - B_2\left(\hat{\bar{x}}\right)\right) + \bar{L}\left(B_1\left(\hat{\bar{x}}\right) - B_1(\bar{x})\right)\right]u.\end{aligned} \tag{14}$$

Additionally, suppose that for (14) the following relations are satisfied in a local region around $\bar{x}$ and $\hat{\bar{x}}$ as

$$\begin{aligned}&\Big\|\left[\left(A_{21}(\bar{x}) - A_{21}\left(\hat{\bar{x}}\right)\right)\right. \\ &\quad \left. + \bar{L}\left(A_{11}(\bar{x}) - A_{11}\left(\hat{\bar{x}}\right)\right)\right]y_m\Big\| \leq \gamma_1\|e\|; \\ &\Big\|\left[\left(B_2(\bar{x}) - B_2\left(\hat{\bar{x}}\right)\right)\right. \\ &\quad \left. + \bar{L}\left(B_1(\bar{x}) - B_1\left(\hat{\bar{x}}\right)\right)\right]u\Big\| \leq \left(\gamma_2 + \gamma_3\|u\|\right)\|e\|\end{aligned} \tag{15}$$

where γ_1 and γ_2 are nonnegative constants.

By taking into account (14) and (15), the reduced-order observer design is based on the following assumptions.

H1. Matrices $A_{12}(\bar{x})$ and $A_{22}(\bar{x})$ in (14) depend only on state $\bar{x}_1$, and inequalities in (15) are satisfied.

H2. Consider that matrices $A_{ij}(\bar{x}) = A_{ij}\left(\bar{x}_1\right)$ and $B_i(\bar{x}) = B_i\left(\bar{x}_1\right)$.

Assumption **H1** considers that the entries of $A_{12}(\bar{x})$ and $A_{22}(\bar{x})$ depend on the system measured variables, where such a fact is directly related to the system one deals with; such requirement could be fulfilled for nonlinear systems with the SDCF representation because of its different state-dependent factorization possibilities [7,21], while inequalities in (15) consider the possible differences between the observer and the system matrices, which can lead to local results in the observer design. On the other hand, assumption **H2** considers the case where all the state-dependent matrices depend only on measured variables (or even constant matrices), then the observer design is simplified, as stated in Corollary 1.

At this point, the main contribution of the paper is established as follows.

Theorem 1. Consider that system (1) can be presented in the SDCF form as in (3) and that (8) is observable. Assume that **H1** is fulfilled. If for a given gain matrix $\bar{L}$ and a positive constant κ there exists a positive definite symmetric matrix W which satisfies

$$\begin{aligned}&W\left(A_{22}(\bar{x}) - \bar{L}A_{12}(\bar{x})\right) \\ &\quad + \left(A_{22}(\bar{x}) - \bar{L}A_{12}(\bar{x})\right)^T W \leq -\kappa I_{n-q}\end{aligned} \tag{16}$$

with

$$\kappa > 2\left(\gamma_1 + \gamma_2 + \gamma_3\|u\|\right)\|W\| \tag{17}$$

then the estimation error (13) converges asymptotically to zero, where I_{n-q} is the $(n-q)\times(n-q)$ identity matrix. Moreover, if all assumptions hold globally, then the estimation error converges globally asymptotically to zero.

Proof. See Appendix A.

Note that the relations between (16) and (17) ensure the estimation error stability in accordance with the stability analysis carried out in the theorem proof (appendix A). *A posteriori* in subsection 4.3.2, such error stability is also analyzed through the state-dependent eigenvalues determination, while inequality (16) is numerically verified for the LIM application.

In addition to the stated in Theorem 1, suppose that once factorized $f(x)$ in (3) the assumption **H2** is fulfilled, then the following result can be derived.

Corollary 1. Suppose that **H2** holds. If for a given gain matrix $\bar{L}$ and a positive constant κ there exists a positive definite symmetric matrix W which satisfies inequality (16), then the estimation error converges asymptotically to zero.

Proof. See Appendix B.

Note that in the analysis of the observer convergence, the norm of the control input $\|u\|$ in (15) and (17) appears because of the differences between the matrices $B_i\left(\hat{\bar{x}}\right)$ and $B_i(\bar{x})$, which avoid the elimination of the control input dependence and can lead to local results in Theorem 1. The requirement of such norm is overcome when $B_i\left(\hat{\bar{x}}\right) = B_i(\bar{x}) = B_i\left(\bar{x}_1\right)$, that is, when these matrices are state-dependent on measured variables, which correspond to the result of Corollary 1.

Remark 1. It is worth remarking that the proposed observer synthesis can be performed for those nonlinear systems with the SDCF structure, the characteristics of which can be found in different real systems [8–14]. Moreover, this salient feature is used in this paper to obtain the solution for the optimal tracking control, as follows.

III. OPTIMAL TRACKING CONTROL FOR SDCF NONLINEAR SYSTEMS

As an application of the proposed reduced-order observer, this section uses the estimated states for the optimal tracking control. In this sense, the optimal tracking control solution is stated for SDCF nonlinear systems, as proposed in [11], under the assumption that the full state x is available for feedback; nevertheless, this assumption is often unrealistic since frequently there are fewer measured variables (y_m) than system state variables, where the remaining ones need to be estimated. Hence, once the unmeasured variables are estimated, they are used in combination with the measured ones for the implementation of the feedback optimal controller.

With respect to the optimal tracking control, the output of the system is required to track a desired trajectory as closely as possible in an optimal sense and with minimum control effort expenditure [26–28]. The optimal tracking scheme arises for many applications, such as aerospace, electrical machines, robotics, among others.

In order to introduce optimal tracking, let us define for system (3) its respective output to be controlled as

$$y = C(x)\,x \tag{18}$$

while the tracking error is defined as

$$\begin{aligned} \varepsilon &= r - y \\ &= r - C(x)\,x \end{aligned} \tag{19}$$

where r is the desired reference to be tracked by the system output y.

The quadratic cost functional J to be minimized, associated with system (3), is defined as

$$J = \frac{1}{2}\int_{t_0}^{\infty} \left(\varepsilon^T Q\,\varepsilon + u^T R\,u\right)\,dt \tag{20}$$

where Q and R are symmetric and positive definite matrices. Therefore, the optimal tracking solution is related to determining the control $u(t),\ t \in [t_0, \infty)$, such that the criterion (20) is minimized.

It is worth noting that y in (18) corresponds to the (possibly nonlinear) system output to be controlled, whereas y_m in (2) represents the (usually linear) system measured variables used for the observer synthesis.

3.1 Optimal tracking controller

Let us assume that the state variables are available for feedback (from measurements and the reduced-order observer). Under this condition the optimal tracking control solution is developed in [11] and extended in [15] for the case in which a disturbance is affecting the system. The optimal tracking control proposed in [11] (Theorem 2) establishes that for a state-dependent controllable and observable system (3) with (18), the optimal controller

$$u^*(x) = -R^{-1}B^T(x)\,\left(P(x)\,x - z(x)\right) \tag{21}$$

achieves trajectory tracking for the system along a desired trajectory r, where $P(x)$ is the solution of

$$\begin{aligned} \dot{P}(x) = &-C^T(x)\,Q\,C(x) + P(x)\,B(x)\,R^{-1}\,B^T(x) \\ &\times\, P(x) - A^T(x)\,P(x) - P(x)\,A(x) \end{aligned} \tag{22}$$

and $z(x)$ is the solution of

$$\begin{aligned} \dot{z}(x) = &-\left[A(x) - B(x)\,R^{-1}B^T(x)\,P(x)\right]^T z(x) \\ &- C^T(x)\,Q\,r \end{aligned} \tag{23}$$

with boundary conditions $P(x(\infty)) = 0$ and $z(x(\infty)) = 0$, respectively*.

* Please note that in [11] (Theorem 2), there is performed a simplification in the notation, nonetheless, the full notation is $P(x(\infty)) = 0$ and $z(x(\infty)) = 0$.

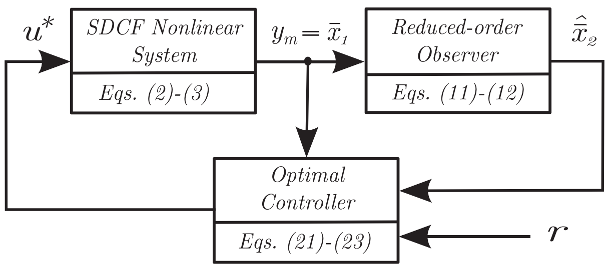

Fig. 1. Observer-based optimal tracking control scheme.

Remark 2. Notice the motions of P and z, that is, the motions of differential Riccati Eq. (22) and differential vector (23), are time-depending, that is $P(t)$ and $z(t)$, and are only state-dependent functions in accordance with their respective right-hand side through matrices $A(x)$, $B(x)$ and $C(x)$, as proposed and developed in [29], in which a state-dependent differential Riccati equation is solved instead of solving an algebraic one. Such state dependences are denoted in this paper and in [11] as $P(x)$ and $z(x)$, respectively.

The resulting control law (21) is optimal in the sense that it minimizes the cost functional (20). Additional details of the controller design can be seen in [11]. It is worth mentioning that different works have taken advantage of the state-dependent Riccati Eq. (22) in the analysis and synthesis of nonlinear optimal control methodologies and their applications [30–34].

Based on the separation principle [35,36], the design of the optimal tracking controller for SDCF nonlinear systems is combined with the state-dependent reduced-order observer, established by (11)– (12). The complete control scheme for achieving the optimal tracking control in combination with the proposed observer is illustrated in Fig. 1.

IV. REAL-TIME APPLICATION FOR THE LIM

This section illustrates the real-time applicability of the proposed observer synthesis and optimal tracking control for the LIM, with a dynamical model that can be described as a multiple-input multiple-output SDCF nonlinear system. The LIM is a special electrical machine in which the electrical energy is directly converted into mechanical energy of translatory motion. This system has found its applications in transportation, industry, automation, and home appliances [37,38], among others, where a linear motion is required. The LIM has many excellent performance features, such as high-starting thrust force, elimination of gears between motor and motion devices, reduction of mechanical losses and the size of motion devices, high-speed operation and silence [37,39].

4.1 Linear induction motor prototype description

The plant for applying the observer-controller is the LIM LabVolt model 8228 (trademark of LabVolt®), shown in Fig. 2. In accordance with the user manual [40], the movable part corresponds to the stator, which is made of an iron core and windings on 18 *mm* polyvinyl chloride blocks mounted on bearing rollers, while the rotor is a 2 *m* rail made of an iron support and an aluminum plate. In the LIM, the stator is excited by a three-phase power supply such that a traveling flux is generated in the stator and induced into the rotor, producing the respective induced currents in the rotor (also named Foucault currents), then a force is originated to generate the linear movement [38]. Fig. 3a depicts the connection scheme between the different devices for the linear induction motor prototype. The personal computer includes the necessary software for the algorithms' implementation and for the transmission of the information to the data acquisition board. The corresponding control signals are applied to the power converter module (Fig. 3b), which transforms them into the adequate control inputs (via a PWM strategy) for the LIM. The position and the currents measurements are also transmitted to the data acquisition board to obtain a closed-loop system. The algorithms are implemented in the data acquisition and control board DS1104 (trademark of dSpace GmbH). This board permits downloading applications directly from Simulink (MathWorks Inc®).

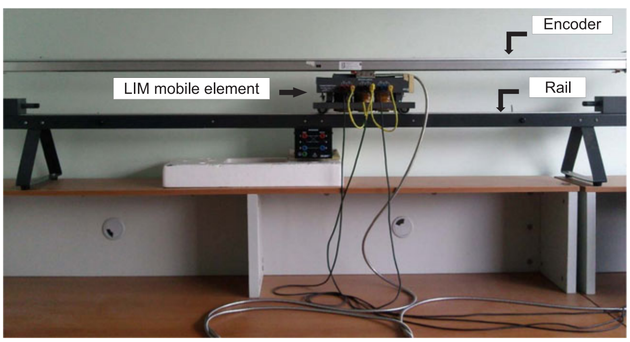

Fig. 2. Linear induction motor system. [Color figure can be viewed at wileyonlinelibrary.com]

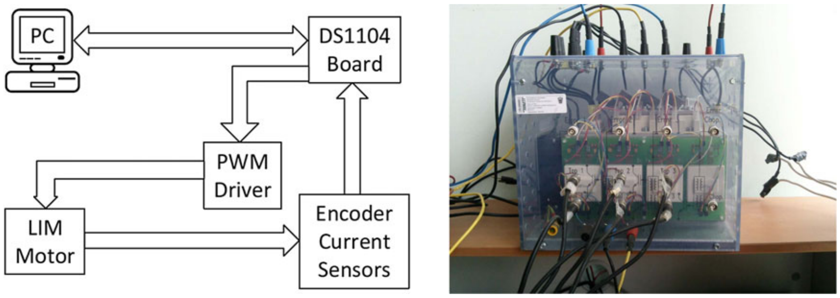

(a) Prototype block diagram. (b) IGBT converter module.

Fig. 3. LIM prototype description. [Color figure can be viewed at wileyonlinelibrary.com]

4.2 Linear induction motor model

The LIM in the $\alpha - \beta$ frame is described by the following nonlinear system [41]:

$$
\begin{aligned}
\frac{d\,q_m}{d\,t} &= v \\
\frac{d\,v}{d\,t} &= -k_1\big(i_\alpha\left(\lambda_\alpha \sin\left(n_p\,q_m\right) + \lambda_\beta \cos\left(n_p\,q_m\right)\right) \\
&\quad + i_\beta\left(\lambda_\beta \sin\left(n_p\,q_m\right) - \lambda_\alpha \cos\left(n_p\,q_m\right)\right)\big) - k_2 v \\
\frac{d\,\lambda_\alpha}{d\,t} &= -k_4\left(i_\alpha \sin\left(n_p\,q_m\right) - i_\beta \cos\left(n_p\,q_m\right)\right) \\
&\quad + k_4 v\left(i_\alpha \sin\left(n_p\,q_m\right) - i_\beta \cos\left(n_p\,q_m\right)\right) \\
&\quad + k_5\left(i_\alpha \cos\left(n_p\,q_m\right) + i_\beta \sin\left(n_p\,q_m\right)\right) - k_6\lambda_\alpha \\
\frac{d\,\lambda_\beta}{d\,t} &= k_5\left(\cos\left(n_p\,q_m\right) i_\beta - \sin\left(n_p\,q_m\right) i_\alpha\right) \\
&\quad - k_4\left(\cos\left(n_p\,q_m\right) i_\alpha + \sin\left(n_p\,q_m\right) i_\beta\right) \\
&\quad + k_4 v\left(\cos\left(n_p\,q_m\right) i_\alpha + \sin\left(n_p\,q_m\right) i_\beta\right) - k_6\lambda_\beta \\
\frac{d\,i_\alpha}{d\,t} &= k_9 i_\alpha - k_{10} u_\alpha + k_8 v\big(-\sin\left(n_p\,q_m\right)\lambda_\alpha \\
&\quad - \cos\left(n_p\,q_m\right)\lambda_\beta\big) - k_7\big(\cos\left(n_p\,q_m\right)\lambda_\alpha \\
&\quad - \sin\left(n_p\,q_m\right)\lambda_\beta\big) \\
\frac{d\,i_\beta}{d\,t} &= k_9 i_\beta - k_{10} u_\beta - k_7\big(\sin\left(n_p\,q_m\right)\lambda_\alpha \\
&\quad + \cos\left(n_p\,q_m\right)\lambda_\beta\big) + k_8 v\big(\cos\left(n_p\,q_m\right)\lambda_\alpha \\
&\quad - \sin\left(n_p\,q_m\right)\lambda_\beta\big)
\end{aligned}
\tag{24}
$$

with

$$k_1 = \frac{L_{sr} n_p}{D_m L_r}; \qquad k_2 = \frac{R_m}{D_m}; \qquad k_3 = \frac{1}{D_m};$$

$$k_4 = L_{sr} n_p; \qquad k_5 = \frac{L_{sr} R_r}{L_r}; \qquad k_6 = \frac{R_r}{L_r};$$

$$k_7 = \frac{L_{sr} R_r}{L_r\left(L_{sr}^2 - L_r L_s\right)}; \qquad k_8 = \frac{L_{sr} n_p}{L_{sr}^2 - L_r L_s};$$

$$k_9 = \frac{L_r^2 R_s + L_{sr}^2 R_r}{L_r\left(L_{sr}^2 - L_r L_s\right)}; \qquad k_{10} = \frac{L_r}{L_{sr}^2 - L_r L_s}$$

where q_m is the position, v is the linear velocity, λ_α and λ_β are the rotor fluxes, i_α and i_β are the stator currents, and u_α and u_β are the voltages. Parameter R_s is the winding resistance per phase, R_r is the secondary resistance per phase, L_{sr} is the maximum mutual inductance between stator and rotor, L_s is the primary inductance per phase, L_r is the secondary inductance per phase, R_m is the viscous friction and iron-loss coefficient, D_m is the mass of the moving element and n_p is the number of poles' pairs. The parameters of the plant are $R_s = 5.3\,\Omega$, $L_s = 28\,mH$, $R_r = 3.5\,\Omega$, $L_r = 28\,mH$, $L_{sr} = 24\,mH$, $D_m = 2.7\,kg$, $R_m = 36\,kg/s$, and $n_p = 4$.

$$
A(x) = \begin{bmatrix}
0 & 1 & 0 & 0 & 0 & 0 \\
0 & -k_2 & k_1\rho_2(x_1)x_6 - k_1\rho_1(x_1)x_5 & -k_1\rho_2(x_1)x_5 - k_1\rho_1(x_1)x_6 & 0 & 0 \\
0 & k_4\left(\rho_1(x_1)x_5 - \rho_2(x_1)x_6\right) & -k_6 & 0 & k_5\rho_2(x_1) - k_4\rho_1(x_1) & k_5\rho_1(x_1) + k_4\rho_2(x_1) \\
0 & k_4\left(\rho_2(x_1)x_5 + \rho_1(x_1)x_6\right) & 0 & -k_6 k_7\rho_1(x_1) - k_8\rho_2(x_1)x_2 & -k_5\rho_1(x_1) - k_4\rho_2(x_1) & k_5\rho_2(x_1) - k_4\rho_1(x_1) \\
0 & 0 & -k_7\rho_2(x_1) - k_8\rho_1(x_1)x_2 & -k_7\rho_2(x_1) - k_8\rho_1(x_1)x_2 & k_9 & 0 \\
0 & 0 & k_8\rho_2(x_1)x_2 - k_7\rho_1(x_1) & & 0 & k_9
\end{bmatrix};
$$

The system outputs to be controlled are the position q_m and the flux squared module (typically used to maximize the motor efficiency [42]), which are defined respectively as

$$y_1 = q_m$$

$$y_2 = \lambda_\alpha^2 + \lambda_\beta^2.$$

By defining the state vector and the control input as

$$x = \begin{bmatrix} x_1 \\ x_2 \\ x_3 \\ x_4 \\ x_5 \\ x_6 \end{bmatrix} = \begin{bmatrix} q_m \\ v \\ \lambda_\alpha \\ \lambda_\beta \\ i_\alpha \\ i_\beta \end{bmatrix}; \qquad u = \begin{bmatrix} u_\alpha \\ u_\beta \end{bmatrix}$$

system (24) can then be rewritten as

$$\begin{aligned} \dot{x} &= A(x)\,x + B(x)\,u \\ y &= C(x)\,x \end{aligned} \tag{25}$$

where $A(x)$ is defined at the bottom of the previous page, with $\rho_1(x_1) = \sin\left(n_p x_1\right)$ and $\rho_2(x_1) = \cos\left(n_p x_1\right)$,

$$B(x) = \begin{bmatrix} 0 & 0 \\ 0 & 0 \\ 0 & 0 \\ 0 & 0 \\ -k_{10} & 0 \\ 0 & -k_{10} \end{bmatrix}; \quad C^T(x) = \begin{bmatrix} 1 & 0 \\ 0 & 0 \\ 0 & x_3 \\ 0 & x_4 \\ 0 & 0 \\ 0 & 0 \end{bmatrix}.$$

We remark that the SDCF structure in (25) is rather general for industrial applications, and the state-dependence in the associated matrices $A(x)$, $B(x)$ and $C(x)$ rely on each particular system, where some of those matrices could be state-independent (i.e., constant matrices). Apart from the LIM system presented for the case study in this paper, other practical nonlinear components related to power systems can be modeled with the SDCF representation; for instance, the doubly-fed induction generator [11], the synchronous generator [12], three-phase back-to-back power converters [43], biomedical applications [44], among others. Therefore, the real-time implementation of state feedback controllers for these systems requires adequate observers with the aim of reducing implementation costs and of estimating variables that are difficult to measure.

4.3 Reduced-order observer synthesis for the LIM

In applications where a state-feedback controller is desired to be implemented, the design of observers to estimate the unmeasured variables is usually necessary [23,45–47]. In this case for the LIM, assume that the linear position q_m, the linear velocity v, the stator currents $\left(i_\alpha,\, i_\beta\right)$, and the input voltages $\left(u_\alpha,\, u_\beta\right)$ are available from measurements; therefore, matrix H related to the measured variables in (2) is given as

$$H = \begin{bmatrix} 1 & 0 & 0 & 0 & 0 & 0 \\ 0 & 1 & 0 & 0 & 0 & 0 \\ 0 & 0 & 0 & 0 & 1 & 0 \\ 0 & 0 & 0 & 0 & 0 & 1 \end{bmatrix}$$

and hence $n = 6$ and $q = 4$. A state feedback control synthesis, however, cannot be performed since the rotor fluxes are not available, and they are not easy to measure. Therefore, it is reasonable to synthesize a reduced-order observer to estimate the rotor fluxes $\left(\lambda_\alpha,\, \lambda_\beta\right)$ as follows.

4.3.1 Transformed induction motor model

In accordance with Section II, the nonsingular transformation matrix T is determined as

$$T = \begin{bmatrix} H \\ S \end{bmatrix} = \begin{bmatrix} 1 & 0 & 0 & 0 & 0 & 0 \\ 0 & 1 & 0 & 0 & 0 & 0 \\ 0 & 0 & 0 & 0 & 1 & 0 \\ 0 & 0 & 0 & 0 & 0 & 1 \\ 0 & 0 & 1 & 0 & 0 & 0 \\ 0 & 0 & 0 & 1 & 0 & 0 \end{bmatrix}$$

where $S = \begin{bmatrix} 0 & 0 & 1 & 0 & 0 & 0 \\ 0 & 0 & 0 & 1 & 0 & 0 \end{bmatrix}$. Thus a system is obtained with the structure given in (5)– (6), with $\bar{x} = \left[\, \bar{x}_1^T \ \bar{x}_2^T \,\right]^T$, where $\bar{x}_1 = \left[\, x_1 \ x_2 \ x_5 \ x_6 \,\right]^T$, $\bar{x}_2 = \left[\, x_3 \ x_4 \,\right]^T$ and

$$A_{11}(\bar{x}) = \begin{bmatrix} 0 & 1 & 0 & 0 \\ 0 & -k_2 & 0 & 0 \\ 0 & 0 & k_9 & 0 \\ 0 & 0 & 0 & k_9 \end{bmatrix}; \quad A_{22}(\bar{x}) = \begin{bmatrix} -k_6 & 0 \\ 0 & -k_6 \end{bmatrix};$$

$$A_{12}(\bar{x}) = \begin{bmatrix} 0 & 0 \\ k_1\rho_2(x_1)x_6 - k_1\rho_1(x_1)x_5 & -k_1\rho_2(x_1)x_5 - k_1\rho_1(x_1)x_6 \\ -k_7\rho_2(x_1) - k_8\rho_1(x_1)x_2 & k_7\rho_1(x_1) - k_8\rho_2(x_1)x_2 \\ k_8\rho_2(x_1)x_2 - k_7\rho_1(x_1) & -k_7\rho_2(x_1) - k_8\rho_1(x_1)x_2 \end{bmatrix};$$

$$A_{21}^T(\bar{x}) = \begin{bmatrix} 0 & 0 \\ k_4\left(\rho_1(x_1)x_5 - \rho_2(x_1)x_6\right) & k_4\left(\rho_2(x_1)x_5 + \rho_1(x_1)x_6\right) \\ k_5\rho_2(x_1) - k_4\rho_1(x_1) & -k_4\rho_2(x_1) - k_5\rho_1(x_1) \\ k_4\rho_2(x_1) + k_5\rho_1(x_1) & k_5\rho_2(x_1) - k_4\rho_1 \end{bmatrix};$$

$$B_1(\bar{x}) = \begin{bmatrix} 0 & 0 \\ 0 & 0 \\ -k_{10} & 0 \\ 0 & -k_{10} \end{bmatrix}; \quad B_2(\bar{x}) = \begin{bmatrix} 0 & 0 \\ 0 & 0 \end{bmatrix}.$$

Note that for the case of the LIM system $A_{11}(\bar{x})$, $A_{22}(\bar{x})$, $B_1(\bar{x})$, and $B_2(\bar{x})$ are constant matrices, and

$A_{12}(\bar{x}) = A_{12}(\bar{x}_1)$ and $A_{21}(\bar{x}) = A_{21}(\bar{x}_1)$. Hence, being that the usage of Theorem 1 or Corollary 1 will depend on the nonlinear system and the obtained SDCF form, the corresponding factorization for the LIM allows the realization of the reduced-order observer in accordance with Corollary 1, where it is required to fulfill (16) to guarantee the observer convergence (giving *a priori* values for $\bar{L}$ and $\kappa > 0$ and finally determining $W > 0$). On the other hand, the values for the parameters γ_1, γ_2 and γ_3 in (15) are not required for the LIM observer design since there are no differences between the corresponding matrices.

For the reduced-order observer, only the state estimation for $\bar{x}_2$ is required, that is, the fluxes λ_α and λ_β, which come from (12) as $\hat{\bar{x}}_2 = \bar{z} + \bar{L}\,y_m$, where $\bar{z}$ is the solution of (11).

4.3.2 Real-time results of the reduced-order observer

Fig. 4 shows the convergence of the observer fluxes to the linear induction motor fluxes. The gain used for the estimator convergence is

$$\bar{L} = \begin{bmatrix} l_{11} & l_{12} & l_{13} & l_{14} \\ l_{21} & l_{22} & l_{23} & l_{24} \end{bmatrix} \tag{26}$$

$$= \begin{bmatrix} 0 & 0 & 0.0001 & 0.0001 \\ 0 & 0 & 0.0001 & -0.0001 \end{bmatrix} \tag{27}$$

which is selected by numerically analyzing the state-dependent eigenvalues for $\left(A_{22}(\bar{x}) - \bar{L}A_{12}(\bar{x})\right)$, where using the plant parameters result in

$$eig = -124.086 \pm 0.5\sqrt{13.6235 + 0.0141566\,x_2^2}$$

which for the operation range of the LIM, the velocity x_2 (in m/s) is low enough to guarantee the eigenvalues negativeness. In addition, since for the LIM the observer design is based on Corollary 1, and by using the gain $\bar{L}$, condition (16) can be verified by selecting (for simplicity) $W = I_2$ and $\kappa = 1$, which must satisfy

$$\begin{aligned} &\left(A_{22}(\bar{x}) - \bar{L}A_{12}(\bar{x})\right) \\ &\quad + \left(A_{22}(\bar{x}) - \bar{L}A_{12}(\bar{x})\right)^T \leq -I_2 \end{aligned} \tag{28}$$

or rewritten as [48]

$$\begin{aligned} &-\left(A_{22}(\bar{x}) - \bar{L}A_{12}(\bar{x})\right) \\ &-\left(A_{22}(\bar{x}) - \bar{L}A_{12}(\bar{x})\right)^T - I_2 \geq 0 \end{aligned} \tag{29}$$

that is, the state-dependent (29) must be a symmetric and positive semidefinite matrix $\forall\,\bar{x}$, for which equivalently its two leading principal minors must be nonnegative $\forall\,\bar{x}$. The minors are numerically evaluated in time and displayed in Fig. 5, which indeed become strictly positive, that is, *Minor* 1 > 0 and *Minor* 2 > 0. Therefore (16) is fulfilled, guaranteeing the observer convergence [49]. Notice that because of the state-dependence in the corresponding matrices, an algebraic verification of (29) is not possible. In this paper such a verification is numerically carried out in time along the system motion.

Fig. 6 displays the control signals used for evaluating the convergence of the proposed observer, where the frequency of the signals is varied to illustrate the effectiveness of the observer. Note that for the LIM observer design, in accordance with Corollary 1, the norm of the control input is not required to achieve the observer convergence since $B_i\left(\hat{\bar{x}}\right) = B_i(\bar{x})$ is a constant matrix. For systems where $B_i\left(\hat{\bar{x}}\right) \neq B_i(\bar{x})$ and an observer-based optimal controller is synthesized, the control signals will remain bounded, which is established in the stability analysis given in the proof of Theorem 2 in [11].

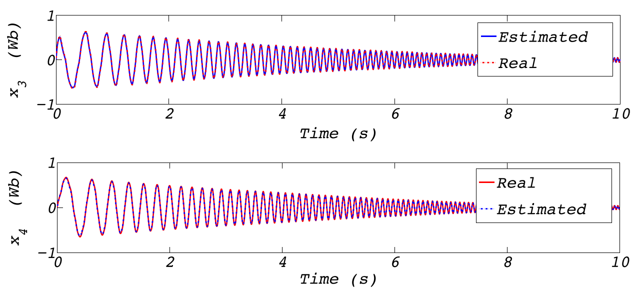

Fig. 4. Estimation for fluxes λ_α and λ_β. [Color figure can be viewed at wileyonlinelibrary.com]

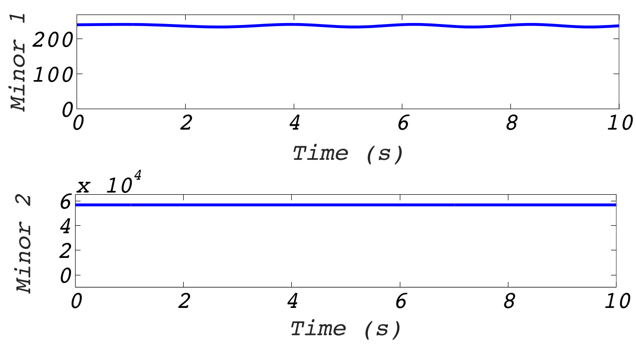

Fig. 5. Minors' positiveness verification. [Color figure can be viewed at wileyonlinelibrary.com]

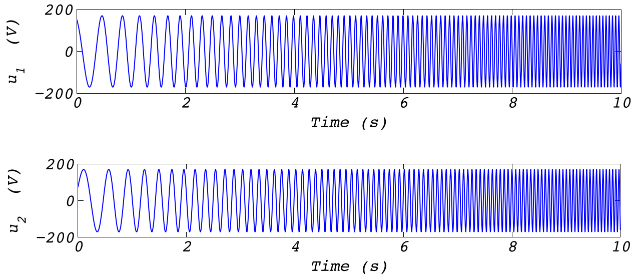

Fig. 6. Input signals for the reduced-order observer evaluation. [Color figure can be viewed at wileyonlinelibrary.com]

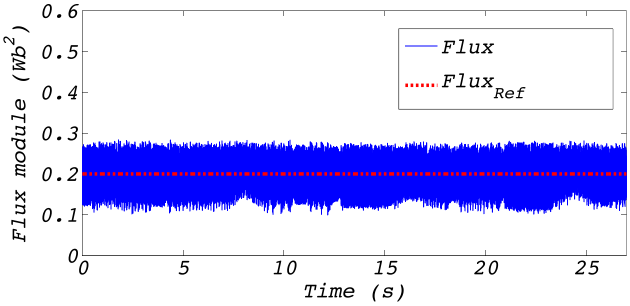

Fig. 8. Optimal tracking for the flux squared module. [Color figure can be viewed at wileyonlinelibrary.com]

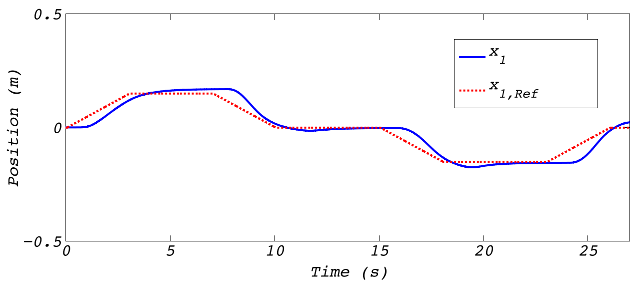

Fig. 7. Optimal tracking for the position control. [Color figure can be viewed at wileyonlinelibrary.com]

4.4 Real-time results of the observer-based optimal tracking controller for the LIM

Since the synthesized optimal controller requires the whole state feedback $\left(q_m, v, \lambda_\alpha, \lambda_\beta, i_\alpha, i_\beta\right)$, the unmeasured variables $\left(\lambda_\alpha, \lambda_\beta\right)$ are obtained from the reduced-order observer.

The results of the position and the flux squared module control are shown in Figs. 7 and 8, respectively, where the tracking for these controlled outputs to the desired references are achieved by using the proposed observer and the optimal control scheme. The reference for the position control $r_1 = x_{1,Ref}$ is a time-varying signal as depicted in Fig. 7, whereas the reference for flux squared module r_2 is $r_2 = Flux_{Ref} = 0.2\ Wb^2$, as displayed in Fig. 8. From the real-time results, it can be noted that the control objectives are achieved in spite of possible parameters' uncertainties, which generally exist in real systems. In this sense, the obtained results could be improved by considering a robust control scheme against parameter uncertainties and external disturbances; moreover, filters for the measured variables could be included to reduce the noise affecting such variables.

The performance of the proposed reduced-order observer-based optimal controller is evaluated in real-time in the LIM prototype. Matrices Q and R for the optimal controller are $Q = diag\{100000, 50000\}$ and $R = diag\{0.001, 0.001\}$, respectively, where these values are selected for achieving an adequate trajectory tracking. Note that matrix Q is a parameter weighting the time evolution of the tracking error e, while R is a matrix weighting the control effort expenditure; hence these matrices are used to establish a trade-off between the tracking performance and the control effort. If more importance is given to the tracking performance, one can select a higher value for Q or reduce R [27], that is, large values for Q will improve the time of the variables' convergence to the desired references, nevertheless, a large control effort will be required; on the other hand, large values for R will minimize the control effort, however, the system variables' time response will be slow and the tracking could not be adequately performed.

V. CONCLUSIONS

This contribution presents a reduced-order observer for SDCF nonlinear systems in order to estimate the unmeasured variables. The estimated states can be used for control purposes such as synthesis of state feedback controllers. The reduced-order observer is illustrated via the implementation in real-time for a linear induction motor, whereby using the estimated states, the trajectory tracking to a desired reference for position and flux squared module is achieved.

REFERENCES

1. Alanis, A. Y., E. Rangel, J. Rivera, N. Arana-Daniel, and C. Lopez-Franco, "Particle swarm based approach of a real-time discrete neural identifier

for linear induction motors," *Math. Probl. Eng.*, Vol. 2013, pp. 1–9 (2013). https://doi.org/10.1155/2013/715094.

2. Banks, H. T., S. C. Beeler, and H. T. Tran, "State estimation and tracking control of nonlinear dynamical systems," *Int. Series of Numerical Math.*, Vol. 143, No. 1, pp. 1–24 (2003).
3. Basin, M. V., *New Trends in Optimal Filtering and Control for Polynomial and Time-Delay Systems*, Springer-Verlag, Berlin (2008).
4. Friedland, B., *Control System Design: An Introduction to State-Space Methods*, McGraw-Hill, New York (1986).
5. Stengel, R. F., *Optimal Control and Estimation*, Dover Publications, Inc, New York (1994).
6. Sundarapandian, V., "Reduced order observer design for nonlinear systems," *Appl. Math. Lett.*, Vol. 19, pp. 936–941 (2006).
7. Cimen, T., "State-dependent Riccati equation (SDRE) control: A survey," *Proc. IFAC 17th World Congr.*, Seoul, Korea, pp. 3761–3775 (2008).
8. Banks, H. T., B. M. Lewis, and H. T. Tran, "Nonlinear feedback controllers and compensators: A state-dependent Riccati equation approach," *Comput. Optim. Appl.*, Vol. 37, No. 2, pp. 177–218 (2007).
9. Chang I. and S.-J. Chung, "Exponential stability region estimates for the state-dependent Riccati equation controllers," *Proc. 48th IEEE Conf.*, Shanghai, China, pp. 1974–1979 (2009).
10. Erdem, E. B., "Analysis and real-time implementation of state-dependent Riccati equation controlled systems," *Ph.D. thesis*, University of Illinois at Urbana-Champaign, Urbana, Illinois (2001).
11. Ornelas-Tellez, F., J. J. Rico, and R. Ruiz-Cruz, "Optimal tracking for state-dependent coefficient factorized nonlinear systems," *Asian J. Control*, Vol. 16, No. 3, pp. 890–903 (2014).
12. Ornelas-Tellez, F., J. J. Rico-Melgoza, and J. J. Rincon-Pasaye, "Optimal control for non-polynomial systems," *J. Frankl. Inst.*, Vol. 350, No. 4, pp. 853–870 (2013).
13. Parrish, D. K. and D. B. Ridgely, "Control of an artificial human pancreas using the SDRE method," *Proc. IEEE Amer. Control Conf.*, Albuquerque, NM, pp. 1059–1060 (1997).
14. Pukdeboon, C., "Optimal output feedback controllers for spacecraft attitude tracking," *Asian J. Control*, Vol. 15, No. 5, pp. 1284–1294 (2013).
15. Ornelas-Tellez, F., J. J. Rico, E. Espinosa-Juarez, and E. N. Sanchez, "Optimal and robust control in DC microgrids," *IEEE Trans. Smart Grid*, Vol. PP, No. 99, pp. 1–12 (2017). https://doi.org/10.1109/TSG.2017.2690566.
16. Cimen, T., "Survey of state-dependent Riccati equation in nonlinear optimal feedback control synthesis," *J. Guid., Control, Dyn.*, Vol. 35, No. 4, pp. 1025–1045 (2012).
17. Mracek, C. P., J. R. Cloutier, and D'Souza. C. A., "A new technique for nonlinear estimation," *Proc. IEEE Int. Conf. Control Applicat.*, Dearborn, MI, pp. 338–343 (1996).
18. Hammett, K. D., C. D. Hall, and D. B. Ridgely, "Controllability issues in nonlinear state dependent Riccati equation control," *J. Guid. Control Dyn.*, Vol. 21, No. 5, pp. 767–773 (1998).
19. Pearson, J. D., "Approximation methods in optimal control I. Sub-optimal control," *J. Electron. Control*, Vol. 13, No. 5, pp. 453–465 (1962).
20. Vidyasagar, M., *Nonlinear Systems Analysis*, SIAM: Society for Industrial and Applied Mathematics, USA (2002).
21. Cloutier, J. R., "State-dependent Riccati equation techniques: An overview," *Proc. 1997 Amer Control Conf*, Albuquerque, NM, pp. 932–936 (1997).
22. Liang, Y.-W. and L.-G. Lin, "Analysis of SDC matrices for successfully implementing the SDRE scheme," *Automatica*, Vol. 49, No. 10, pp. 3120–3124 (2013).
23. Chen, C.-T., *Linear System Theory and Design*, Oxford University Press, New York (1999).
24. Kailath, T., *Linear Systems*, Prentice-Hall, Inc, Englewood Cliffs, NJ (1980).
25. Luenberger, D. G., "Observing the state of a linear system," *IEEE Trans. Military Electronics*, Vol. 8, No. 2, pp. 74–80 (1964).
26. Anderson, B. D. O. and J. B. Moore, *Optimal Control: Linear Quadratic Methods*, Prentice-Hall, Englewood Cliffs, NJ (1990).
27. Athans, M. and P. L. Falb, *Optimal Control: An Introduction to the Theory And Its Applications*, Dover Publications, Inc, Mineola, NY (2007).
28. Alexis, K., G. Nikolakopoulos, and A. Tzes, "On trajectory tracking model predictive control of an unmanned quadrotor helicopter subject to aerodynamic disturbances," *Asian J. Control*, Vol. 16, No. 1, pp. 209–224 (2014).
29. Haessig D. A. and B. Friedland, "State dependent differential Riccati equation for nonlinear estimation and control," *15th IFAC World Congress*, Barcelona, Spain, pp. 8611–8617 (2002).
30. Smidl, V., S. Janous, L. Adam, and Z. Peroutka, "Direct speed control of PMSM drive using SDRE and convex constrained optimization," *IEEE Trans. Ind. Electron.*, Vol. 65, No. 1, pp. 532–542 (2018).
31. Batmani, Y., M. Davoodi, and N. Meskin, "Event-triggered suboptimal tracking controller

design for a class of nonlinear discrete-time systems," *IEEE Trans. Ind. Electron.*, Vol. 64, No. 10, pp. 8079–8087 (2017).
32. Tahirovic, A. and S. Dzuzdanovic, "A globally stabilizing nonlinear model predictive control framework," *IEEE 55th Conf. Decision and Control (CDC)*, Las Vegas, NV, pp. 4033–4039 (2016).
33. Lin, L. G., J. Vandewalle, and Y. W. Liang, "Analytical representation of the state-dependent coefficients in the SDRE/SDDRE scheme for multivariable systems," *Automatica*, Vol. 59, pp. 106–111 (2015).
34. Cimen, T., "Systematic and effective design of nonlinear feedback controllers via the state-dependent Riccati equation (SDRE) method," *Annu. Rev. Control*, Vol. 34, pp. 32–51 (2010).
35. Basin, M., A. G. Loukianov, and M. Hernandez-Gonzalez, "Optimal controller for stochastic polynomial systems with state-dependent polynomial input," *Circuits, Syst. Signal Process.*, Vol. 30, pp. 1463–1479 (2011).
36. Fleming, W. H. and R. W. Rishel, *Deterministic and Stochastic Optimal Control*, Applications of Mathematics, Vol. 1, Springer-Verlag, New York, NY (1975).
37. Boldea, I. and S. A. Nasar, *Linear Electric Actuators and Generators*, Cambridge University Press, Cambridge, Mass (1997).
38. Gieras, J. F., *Linear Inductions Drives*, Oxford University Press, Oxford (1994).
39. Takahashi, I. and Y. Ide, "Decoupling control of thrust and attractive force of a LIM using a space vector control inverter," *IEEE Trans. Ind. Appl.*, Vol. 29, No. 1, pp. 161–167 (1993).
40. LabVolt, *LabVolt 8228 User Manual* (2005).
41. Benitez, V. H., A. G. Loukianov, and E. N. Sanchez, "Neural identification and control of a linear induction motor using an α-β model," Vol. 5, *Proc. Amer. Control Conf.*, Denver, CO, pp. 4041–4046 (2003).
42. Marino, R. and P. Tomei, *Nonlinear Control Design: Geometric, Adaptive and Robust*, Prentice Hall, Hertfordshire (1996).
43. Ruiz-Cruz, R., E. N. Sanchez, F. Ornelas-Tellez, A. G. Loukianov, and R. G. Harley, "Particle swarm optimization for discrete-time inverse optimal control of a doubly-fed induction generator," *IEEE T. Cybern.*, Vol. 43, No. 6, pp. 1698–1709 (2013).
44. Villafuerte, A., F. Ornelas-Tellez, and J. J. Rico-Melgoza, "Adaptive polynomial identification and robust optimal tracking control for nonlinear systems," *Proc. 12th Int. Conf. Elect. Eng. Computing Sci. and Autom. Control (CCE)*, Mexico City, Mexico, pp. 1–6 (2015).
45. Zhang, L., X. Wei, and H. Zhang, "Disturbance observer-based elegant anti-disturbance control for stochastic systems with multiple disturbances," *Asian J. Control*, Vol. 19, pp. 1966–1976 (2017).
46. Sun, T., J. Zhang, and Y. Pan, "Active disturbance rejection control of surface vessels using composite error updated extended state observer," *Asian J. Control*, Vol. 19, No. 5, pp. 1802–1811 (2017).
47. Galvan-Guerra, R., L. Fridman, R. Iriarte, J. E. Velazquez-Velazquez, and M. Steinberger, "Integral sliding-mode observation and control for switched uncertain linear time invariant systems: a robustifying strategy," *Asian J. Control*, pp. 1–15 (2017). https://doi.org/10.1002/asjc.1661.
48. Cloud, M. J., B. C. Drachman, and L. P. Lebedev, *Inequalities with Applications to Engineering*, Springer, New York (2014).
49. Khalil, H. K., *Nonlinear Systems*, Prentice-Hall, Upper Saddle River (1996).

VI. APPENDIX A

6.1 Proof of Theorem 1

Since $A_{12}(\bar{x})$ and $A_{22}(\bar{x})$ only depend on the measured variables $\bar{x}_1$, then $A_{12}(\bar{x}) = A_{12}(\hat{\bar{x}}) = A_{12}(\bar{x}_1)$ and $A_{22}(\bar{x}) = A_{22}(\hat{\bar{x}}) = A_{22}(\bar{x}_1)$; hence the error dynamics (14) becomes

$$\begin{aligned}
\dot{e} &= \left(A_{22}(\bar{x}_1) - \bar{L}A_{12}(\bar{x}_1)\right)\left(\bar{x}_2 - \left(\bar{z} + \bar{L}y_m\right)\right) \\
&\quad + \left[\left(A_{21}(\bar{x}) - A_{21}(\hat{\bar{x}})\right) + \bar{L}\left(A_{11}(\bar{x}) - A_{11}(\hat{\bar{x}})\right)\right] y_m \\
&\quad + \left[\left(B_2(\bar{x}) - B_2(\hat{\bar{x}})\right) + \bar{L}\left(B_1(\bar{x}) - B_1(\hat{\bar{x}})\right)\right] u \\
&= \left(A_{22}(\bar{x}_1) - \bar{L}A_{12}(\bar{x}_1)\right) e \\
&\quad + \left[\left(A_{21}(\bar{x}) - A_{21}(\hat{\bar{x}})\right) + \bar{L}\left(A_{11}(\bar{x}) - A_{11}(\hat{\bar{x}})\right)\right] y_m \\
&\quad + \left[\left(B_2(\bar{x}) - B_2(\hat{\bar{x}})\right) + \bar{L}\left(B_1(\bar{x}) - B_1(\hat{\bar{x}})\right)\right] u.
\end{aligned} \tag{30}$$

In order to analyze the stability of (30), consider the Lyapunov function

$$V(e) = e^T W e, \qquad W = W^T > 0. \tag{31}$$

By taking the time derivative of (31) and after algebraic simplifications, the following is obtained:

$$
\begin{aligned}
\dot{V}(e) &= \dot{e}^T W e + e^T W \dot{e} \\
&= e^T \Big[W \left(A_{22}(\bar{x}) - \bar{L} A_{12}(\bar{x}) \right) \\
&\quad + \left(A_{22}(\bar{x}) - \bar{L} A_{12}(\bar{x}) \right)^T W \Big] e \\
&\quad + 2 e^T W \Big[\left(A_{21}(\bar{x}) - A_{21}\left(\hat{\bar{x}}\right) \right) \\
&\quad + \bar{L} \left(A_{11}(\bar{x}) - A_{11}\left(\hat{\bar{x}}\right) \right) \Big] y_m \\
&\quad + 2 e^T W \Big[\left(B_2(\bar{x}) - B_2\left(\hat{\bar{x}}\right) \right) \\
&\quad + \bar{L} \left(B_1(\bar{x}) - B_1\left(\hat{\bar{x}}\right) \right) \Big] u.
\end{aligned} \tag{32}
$$

By using (15), (16) and (17) in (32), it results in

$$
\begin{aligned}
\dot{V}(e) &\le -\kappa \|e\|^2 + 2\gamma_1 \|W\| \|e\|^2 \\
&\quad + 2(\gamma_2 + \gamma_3 \|u\|) \|W\| \|e\|^2 \\
&= -\left[\kappa - 2\left(\gamma_1 + \gamma_2 + \gamma_3 \|u\| \right) \|W\| \right] \|e\|^2
\end{aligned}
$$

with $\kappa > 2\left(\gamma_1 + \gamma_2 + \gamma_3 \|u\|\right) \|W\|$. Therefore, since $\dot{V}(e)$ is a negative definite function, the estimation error is asymptotically stable [49].

VII. APPENDIX B

7.1 Proof of Corollary 1

It can be directly derived from the proof given for Theorem 1. By considering $A_{ij}(\bar{x}) = A_{ij}\left(\bar{x}_1\right)$ and $B_i(\bar{x}) = B_i\left(\bar{x}_1\right)$, (30) reduces to

$$
\dot{e} = \left(A_{22}\left(\bar{x}_1\right) - \bar{L} A_{12}\left(\bar{x}_1\right) \right) e
$$

and by using (31) as a Lyapunov function, (32) results in

$$
\dot{V}(e) = -\kappa \|e\|^2
$$

with $\kappa > 0$, which is a negative definite function. Thus, e is asymptotically stable.

Fernando Ornelas-Tellez was born in Patzcuaro, Michoacan, Mexico, in 1981. He received HIS B. Sc. degree from Instituto Tecnologico de Morelia (ITM) in 2005, and his M.Sc. and D.Sc. degrees in electrical engineering from the Advanced Studies and Research Center of the National Polytechnic Institute (CINVESTAV-IPN), Guadalajara Campus, in 2008 and 2011, respectively. Since 2012 he has been with Universidad Michoacana de San Nicolas de Hidalgo, where he is currently a professor of Electrical Engineering graduate programs. His research interest centers on optimal control, neural control, sliding modes control and passivity, and their applications to smart grids, power electronics, mechanical systems, and electrical machines.

Alma Y. Alanis was born in Durango, Mexico, in 1980. She received her B. Sc degree from Instituto Tecnologico de Durango (ITD), Durango Campus, Durango, in 2002, and her M.Sc. and the Ph.D. degrees in electrical engineering from the Advanced Studies and Research Center of the National Polytechnic Institute (CINVESTAV-IPN), Guadalajara Campus, Mexico, in 2004 and 2007, respectively. Since 2008 she has been with the University of Guadalajara, where she is currently a Chair Professor in the Department of Computer Science and since 2016 the Dean of the PhD Program of Electronic and Computer Sciences. She is a Senior Member of the IEEE and Subject and Associated Editor of the *Journal of Franklin Institute* (Elsevier) and *Intelligent Automation & Soft Computing* (Taylor & Francis). She is currently serving on a number of IEEE and IFAC Conference Organizing Committees. Her research interest centers on neural control, backstepping control, block control, and their applications to electrical machines, power systems, and robotics.

Jorge D. Rios received his B.Sc. degree in Computer Engineering in 2009 and his M.Sc. degree in Electronics and Computer Engineering in 2014 from University of Guadalajara, and Ph.D. degrees in Electronics and Computer Science at the University of Guadalajara in 2017. His research interest centers on automatic control and intelligent systems.

Mario Graff is a CONACYT Research Fellow working at INFOTEC. He obtained his Ph.D. from the School of Computer Science and Electronic Engineering at the University of Essex, working under the supervision of Professor Riccardo Poli. His research interests are evolutionary computation, genetic programming, machine learning, time series forecasting, and text categorization.